HHS Public Access

Author manuscript

J Mech Behav Biomed Mater. Author manuscript; available in PMC 2016 November 01.

Published in final edited form as:

J Mech Behav Biomed Mater. 2015 November ; 51: 345–355. doi:10.1016/j.jmbbm.2015.07.027.

Compressive fatigue and fracture toughness behavior of injectable, settable bone cements

Andrew J. Harmata[a,b], **Sasidhar Uppuganti**[b,d], **Mathilde Granke**[b,d], **Scott A. Guelcher**[a,b,c], and **Jeffry S. Nyman**[b,c,d,e]

[a]Department of Chemical and Biomolecular Engineering, Vanderbilt University, Nashville, TN, USA

[b]Center for Bone Biology, Vanderbilt University Medical Center, Nashville, TN, USA

[c]Department of Biomedical Engineering, Vanderbilt University, Nashville, TN, USA

[d]Department of Orthopaedic Surgery and Rehabilitation, Vanderbilt University Medical Center, Nashville, TN, USA

[e]Department of Veterans Affairs, Tennessee Valley Healthcare System, Nashville, TN 37212

Abstract

Bone grafts used to repair weight-bearing tibial plateau fractures often experience cyclic loading, and there is a need for bone graft substitutes that prevent failure of fixation and subsequent morbidity. However, the specific mechanical properties required for resorbable grafts to optimize structural compatibility with native bone have yet to be established. While quasi-static tests are utilized to assess weight-bearing ability, compressive strength alone is a poor indicator of *in vivo* performance. In the present study, we investigated the effects of interfacial bonding on material properties under conditions that re-capitulate the cyclic loading associated with weight-bearing fractures. Dynamic compressive fatigue properties of polyurethane (PUR) composites made with either unmodified (U-) or polycaprolactone surface-modified (PCL-) 45S5 bioactive glass (BG) particles were compared to a commercially available calcium sulfate and phosphate-based (CaS/P) bone cement at physiologically relevant stresses (5–30 MPa). Fatigue resistance of PCL-BG/polymer composite was superior to that of U-BG and CaS/P at higher stress levels for each of fatigue failure criteria, related to modulus, creep, and maximum displacement, and was comparable to human trabecular bone. Steady state creep and damage accumulation occurred during the fatigue life of the PCL-BG/PUR and CaS/P cement, whereas creep of U-BG/PUR primarily occurred at a low number of loading cycles. From crack propagation testing, fracture toughness or resistance to crack growth was significantly higher for the PCL-BG composite than

Correspondence to: Jeffry S. Nyman.

Andrew J. Harmata: 107 Olin Hall, 2400 Highland Ave, Nashville, TN 37235, USA. Andrew.J.Harmata@Vanderbilt.edu
Sasidhar Uppuganti: 1215 21st Ave. S., Suite 4200, Nashville, TN 37232, USA, Sasidhar.Uppuganti@Vanderbilt.edu
Mathilde Granke: 1215 21st Ave. S., Suite 4200, Nashville, TN 37232, USA, Mathilde.Granke@Vanderbilt.edu
Scott A. Guelcher: 107 Olin Hall, 2400 Highland Ave, Nashville, TN 37235, USA. Scott.Guelcher@Vanderbilt.edu
Jeffry S. Nyman: 1215 21st Ave. S., Suite 4200, Nashville, TN 37232, USA, Jeffry.S.Nyman@Vanderbilt.edu, (615) 936-6296

for the other materials. Finally, the fatigue and fracture toughness properties were intermediate between those of trabecular and cortical bone. These findings highlight the potential of PCL-BG/polyurethane composites as weight-bearing bone grafts.

Graphical abstract

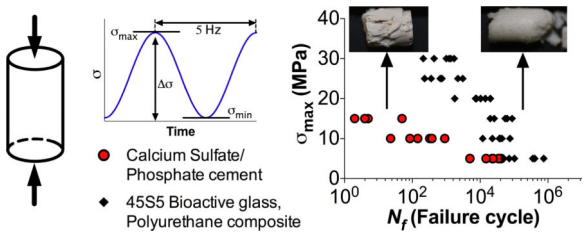

Keywords

synthetic bone graft; polyurethane composite; 45S5 bioactive glass; fatigue; fracture toughness; calcium phosphate bone cement

1. Introduction

Tibial plateau fractures involve a weight-bearing joint and often have depressed portions that require extensive open reduction and internal fixation approaches along with subchondral grafting to maintain articular congruence. Bone grafts utilized in the clinical management of these fractures are subjected to repetitive, dynamic physiological loading from everyday activities, such as sitting, standing, and walking (Ramakrishna, Mayer et al. 2001). Anatomic reduction and maintenance of the joint is important for both bone healing and articular regeneration, since lack of articular congruence after fractures increases the likelihood of osteoarthritis (Anderson, Van Hofwegen et al. 2011). While the use of calcium phosphate cements (CPCs) mitigates the loss of reduction compared to autograft (Simpson and Keating 2004), CPCs are contra-indicated for filling bone voids that are intrinsic to the stability of the bony structure. Consequently, direct reduction of tibial plateau fractures requires stable internal fixation, which is associated with high rates of complications, such as non-union and loss of reduction (Schatzker, McBroom et al. 1976, Young and Barrack 1994, Papagelopoulos, Partsinevelos et al. 2006, Hall, Beuerlein et al. 2009, Musahl, Tarkin et al. 2009). Injectable grafts with bone-like mechanical properties could potentially reduce the amount of internal fixation required and/or allow earlier weight-bearing. Considering that failure of fixation often results in re-hospitalization and an increased risk of poor outcomes (Bosse, MacKenzie et al. 2002), there is a compelling clinical need for weight-bearing bone grafts that prevent failure of fixation and subsequent morbidity.

The criteria for non-resorbable cements designed to maintain the stability of the bony structure have been extensively investigated (Gilbert, Ney et al. 1995, Lewis 2006). Fatigue failure is a predominant *in vivo* failure mode of non-resorbable bone cements used in hip replacements, such as poly(methyl methacrylate) (PMMA) (Ramakrishna, Mayer et al. 2001). Despite the recognized need for resorbable grafts for repair of weight-bearing bone defects (Rezwan, Chen et al. 2006), the specific mechanical properties required for these

materials to optimize structural compatibility with native bone have yet to be established (Ramakrishna, Mayer et al. 2001, Johnson and Herschler 2011). Tensile strength, fracture toughness, and fatigue life have been suggested as key mechanical properties that should be assessed and optimized (Gisep, Kugler et al. 2004, Bohner 2010, Johnson and Herschler 2011). While quasi-static load-to-failure tests in compressive mode are frequently utilized to assess whether a materials is "weight-bearing" (Johnson and Herschler 2011), compressive strength alone is a poor indicator of *in vivo* performance, since physiologic loads typically include shear components and are cyclic (Gisep, Kugler et al. 2004, Bohner 2010). Thus, there is a gap between the methods by which materials are tested and the mechanical environment they encounter post-implantation *in vivo* due to cyclic loading (Bohner 2010).

Reporting only the mean quasi-static strength is often misleading, considering that materials fail under cyclic loads that are below the reported strength of the material (Bohner 2010) (Krause and Mathis 1988). Nonetheless, properties such as fatigue life or fracture toughness are infrequently reported for CPCs or polymer/ceramic composites (Latour and Black 1993, Morgan, Yetkinler et al. 1997, Gisep, Kugler et al. 2004, Johnson and Herschler 2011, Slane, Vivanco et al. 2014). Brittle materials are susceptible to micro-cracking when subjected to repetitive subcritical loading, as is often applied in dynamic fatigue (Morgan, Yetkinler et al. 1997, Kessler, Sottos et al. 2003, Tilbrook, Moon et al. 2005, Pinter, Ladstätter et al. 2006). Micro-crack growth or general damage accumulation can lead to a degradation of material properties that is difficult to detect because it often forms internally within the microstructure. Thus, we considered the assessment of initial fracture toughness and fatigue life at physiologically relevant loads to be a more stringent test (compared to quasi-static methods) of the ability of a bone graft to sustain *in vivo* service loads over time (Morgan, Yetkinler et al. 1997, Gisep, Kugler et al. 2004, Lewis 2006, Bohner 2010).

We recently reported that surface-modification of 45S5 bioactive glass (BG) particles via surface-initiated polymerization of ε-caprolactone significantly increased the initial quasi-static compressive and torsional strength of resorbable lysine-derived polyurethane (PUR) polymer/BG composites to levels exceeding that of human trabecular bone (Harmata, Ward et al. 2014). In the present study, we investigated the effects of interfacial bonding on material properties under conditions that re-capitulate the cyclic loading associated with tibial plateau and other weight-bearing fractures (Gisep, Kugler et al. 2004, Bohner 2010). We evaluated the initial cyclic compressive fatigue properties of PUR polymer/BG composites when subjected to physiological (5–15 MPa) (Ramakrishna, Mayer et al. 2001, ASTM 2010) or supra-physiological (15–30 MPa) loads. Experimental composites were compared to a commercially available, resorbable, and biphasic CPC (CaS/P), which has been reported to support rapid remodeling and an early return to weight-bearing activities when used to reconstruct bone voids following intra-lesional curettage of primary benign bone tumors (Evaniew, Tan et al. 2013). Furthermore, the selected biphasic CPC has similar compressive properties to those of monophasic apatitic cements (Dumas, BrownBaer et al. 2012, Dumas, Prieto et al. 2014). The fatigue life (N_f) was determined for three independent definitions of failure, which were chosen to represent three potential mechanisms of clinical failure, including accumulation of internal micro-crack defects, plastic deformation, and subsidence. In order to evaluate the ability of the composites to resist crack growth, fracture

toughness testing of single edge-notched beam specimens in mode I was conducted. The stress intensity factor (K) and J-integral values were calculated to determine the toughness to initiate cracking and the additional contribution of inelastic deformation (e.g., plasticity) as well as the toughness of a growing crack, respectively (Ritchie, Koester et al. 2008).

2. Materials and methods

2.1 Materials

Melt-derived 45S5 bioactive glass particles (150–212 μm diameter) were purchased from Mo-Sci Corp. (Rolla, MO). (3-Aminopropyl)triethoxyilane (APTES) and ε-caprolactone were purchased from Sigma-Aldrich (St. Louis, MO). Magnesium sulfate, stannous octoate ($Sn(Oct)_2$), and phosphate-buffered saline (PBS) were acquired from Thermo Fisher Scientific (Waltham, MA). Triethylenediamine (TEDA) was purchased from Evonik (Parsipanny, NJ). A lysine triisocyanate (LTI)-polyethylene glycol (PEG) prepolymer (21% NCO) was supplied by Medtronic (Memphis, TN). $_{D,L}$-lactide and glycolide were supplied by Polysciences (Warrington, PA). Polyester triol of 300 Da was synthesized with a backbone comprising 70% ε-caprolactone, 20% glycolide, and 10% $_{D,L}$-lactide (T7C2G1L300). Commercially available PRO-DENSE®, a biphasic bone cement composed of calcium sulfate and calcium phosphate (CaS/P) was obtained from Wright Medical (Memphis, TN). PRO-DENSE® comprises 75% $CaSO_4$ and 25% $CaPO_4$ (brushite and granular tricalcium phosphate).

2.2 Preparation of experimental specimens

The study design included comparing the fatigue life of three synthetic bone grafts at multiple stress levels, although not all materials could withstand more than 1 cycle at higher levels (Table 1). BG particles ranging from 150–212 μm diameter were used, since this size range has been reported to enhance new bone formation (Chan, Thompson et al. 2002, Malinin, Carpenter et al. 2007, Dumas, Davis et al. 2010). The two BG/polyurethane (PUR) composites investigated incorporated either: (a) cleaned and unmodified BG particles (U-BG), or (b) cleaned BG particles subsequently modified by surface-initialed polymerization of ε-caprolactone (PCL-BG) (Harmata, Ward et al. 2014). For cleaning, BG particles were sonicated for 5 min in a solution of acetone and deionized (DI) water (5/95 by volume %, respectively) at room temperature, followed by rinsing in DI water under sonication for 5 min (Verne, Vitale-Brovarone et al. 2009). A total of three washing cycles were performed. PCL-BG were modified by adsoprtion of APTES molecules, incubated in a 2 μM solution of APTES in 9:1 (v/v) ethanol:DI water for 5 h at room temperature (Jiang, Walker et al. 2005, Harmata, Ward et al. 2014), and annealed at 100°C for 1 h, followed by ring-opening polymerization (ROP) ε-caprolactone. A mixture comprising a 1:1000 molar ratio of $Sn(Oct)_2$: ε-caprolactone(Jiang, Walker et al. 2005) and a 0.83:1 weight ratio of Sil-BG: ε-caprolactone was reacted with silane-modified BG particles while stirring at 110°C for 24h. The resulting PCL-BG particles were extracted with chloroform to remove non-grafted PCL and dried at 40°C for 24 h (Harmata, Ward et al. 2014).

BG/polymer composites were prepared by mixing the LTI-PEG prepolymer, polyester triol, BG particles, and TEDA catalyst as previously described (Harmata, Ward et al. 2014). The

relative amounts of LTI-PEG prepolymer and polyol were calculated assuming an isocyanate index of 140 (i.e., 40% excess isocyanate) (Guelcher, Patel et al. 2006). The amount of BG was based on a density of 2.7 g cm^{-3} and a targeted volume percent (56.7%) in the final composite. All components were hand-mixed, loaded into a 1 mL syringe, and injected into a mold at room temperature and 40–50% relative humidity.

Composites created for compressive fatigue testing were injected into a cylindrical mold (6 mm diameter) and cured under a load of 0.96 kg for 5 min to simulate compaction of the material in a confined defect space. Composites were further cured at 37°C for 24 h while not loaded. After curing, the ends of the composites were cut to ensure parallel faces and a length:diameter ratio of 2:1. Composites created for fracture toughness testing were injected into a rectangular metal mold with dimensions 7.4 mm × 3.7 mm × 36.9 mm ($W \times B \times L$), with $B = 0.5W$, as per the fracture toughness test standard ASTM E1820 [1]. To fabricate the commercially available CaS/P cement specimen, the mixing protocol provided in a 20 CC kit was followed. The mixed CaS/P paste was injected into the same cylindrical or rectangular mold as the BG/PUR composites, allowed to cure at 37°C for 24 h, and cut in the same fashions. All specimens were conditioned in PBS at room temperature for 24 h immediately before testing. While the calcium sulfate component in the CaS/P is soluble in water, the mass loss of the CaS/P cement after 1 day under accelerated conditions has been reported as <5% (Moseley and Blum 2008), and thus the effect of calcium sulfate dissolution on mechanical properties was considered to be modest.

2.3 Compressive fatigue mechanical testing

Following ASTM F2118-10, cylindrical specimens were loaded in dynamic compressive fatigue using a servohydraulic material testing instrument (MTS 858 Bionix, Eden Prairie, MN). Compressive fatigue was employed because bone grafts are primarily subjected to compression *in vivo*. Specimens were loosely wrapped in medical gauze in order to distribute and maintain constant hydration during testing, as adapted from previous methods (Caler and Carter 1989). Specimens were placed between two rigid compression platens. The upper platen, which was attached to the actuator, was lowered until it made contact with the specimen as determined by a detected force of 1 N transmitted through the lower stationary platen attached to a load cell (Tovey Engineering Inc., SWT14-5K-000, with a maximum capacity of 14 kN). A calibrated MTS extensometer (634.31F-24) with a gage length of 20 mm was attached to both platens, via knife-edges with a V-notch and silicon elastic bands, to track the overall strain experienced by the specimens. Specimens were cyclic-loaded in sinusoidal compressive testing under load control at a frequency of 5 Hz (Slane, Vivanco et al. 2014). Specimens were loaded from the nominal compressive preload (minimum stress of 0.03 MPa) to a varied maximum stress level (σ_{max}), from 5 to 30 MPa (Table 1), which correspond to physiologically relevant service loads. All testing was performed at room temperature and specimens irrigated with water via a drip-system to maintain hydration and ambient temperature. When the overall strain on the specimen reached 5% or it reached 1 million load cycles, whichever occurred first, the specimen was unloaded and the testing was stopped. The MTS material testing instrument was tuned (adjusting Proportional, Integral, and Derivative terms) for each of the material to ensure that the cyclic loading sine wave reached the maximum stress (peak) and minimum stress

(valley) levels. The same tuning parameters were applied to all the specimens tested within each group.

During the cyclic testing, the force vs. displacement data were recorded for the first cycle and then for one complete cycle at intervals determined by projected fatigue life (Table 1). The MTS control software acquired data at 50 Hz for the test parameters of load, displacement, strain and number of load cycles. The following properties were then calculated using standard mechanical equations for fatigue testing of cylindrical specimens. The compressive engineering stress (σ) was calculated by dividing the load by the cross sectional area of the samples post-hydration. Secant modulus (E) was defined as the ratio in change in stress ($\Delta\sigma$) by change in strain ($\Delta\varepsilon$) (Fig. 1). The number of cycles (N), overall creep strain (relative to initial strain) (c_k), loading secant modulus (E), and maximum displacement (d_m) were measured for each specimen (Fig. 1). Mechanical fatigue failure was defined based on three different criteria: 1) 10% decrease in secant modulus, 2) 1% creep deformation (c_k), and 3) 3% maximum displacement (d_m). The initial modulus was defined as the average of the moduli of the first 10 cycle intervals (Table 1), when >10 intervals occurred, otherwise the modulus of the first cycle interval. Cycle intervals were defined differently for each material based on projected fatigue failure. The strains c_k and d_m were defined based on the initial height of the specimen (set as the maximum potential c_k and d_m). The three failure definitions were chosen to represent three potential mechanisms of clinical failure, accumulation of internal crack defects, plastic deformation, and subsidence. The fatigue life (N_f) was defined as the number of cycles achieved until mechanical failure per definition. The run-out maximum for N_f was set at 1 million cycles. The mean fatigue life of groups at each corresponding stress level were statistically compared by individual t-tests utilizing nonparametric setting with Mann-Whitney test.

2.4 Fracture toughness mechanical testing

After removing materials from the rectangular molds (size and fabrication method described above), single-edge notched beam (SENB) specimens were created using a low-speed diamond wheel saw (SouthBay Technology Inc.) and sharpened further into a pre-crack by means of a razor blade lubricated with 1 μm Buehler MetaDi diamond particulate solution to give original crack size a_0 = 1.4–2.2 mm (approximately 0.25W). The a_0 length was chosen (as compared to a_0 = 0.5W, as required by ASTM E1820) in order to provide greater opportunity for more stable cracking events in the brittle materials. A VanGuard 12424MM series confocal microscope, at 10X magnification, measured the exact length of the starter notch. After positioning the SENB specimens horizontally on two 1 mm diameter supports with a ~30 mm span S (equal to 4×W), they were loaded mid-span (in-line opposite to the notch) in three-point bending clamps (Instron Fixtures Series 2810-413) using another axial servo-hydraulic testing system (DynaMight 8841, Instron, Norwood, MA) with 1 kN load cell (Honeywell). With this mode of crack surface displacement (Mode I), tensile loading is exerted on the specimen such that crack propagates as the crack faces move apart. The force vs. displacement (LVDT) data were recorded at 50 Hz as the specimen was tested in displacement control to failure with a progressive, multiple loading (+0.07 mm at 0.01 mm/s)-unloading (−0.04 mm at 0.015 mm/s)-dwell scheme (rising R-curve approach). The time between load/unload sequence was kept as short as possible while allowing sufficient

time to adjust the macro focus of the camera macro lens and take a picture of the imparted crack propagation. All testing was performed at room temperature.

The bone cement and composites exhibit non-linear mechanical behavior (i.e., a significant amount of plastic deformation). Thus, the fracture behavior of these materials was studied in the framework of elastic-plastic fracture mechanics. The fracture resistance was characterized in terms of the *J*-integral for all groups tested, without the correction of crack extension (i.e. crack lengths (*a*) = initial crack length (a_0)). The value of *J* was calculated for each cycle by adding its elastic and plastic components:

$$J=\frac{K^2(1-v^2)}{E}+J_{pl} \quad (1)$$

.

The critical stress intensity required to initiate cracks (K_{init}) was computed as $K_{init}=\sqrt{\frac{J\cdot E}{1-v^2}}$ at the maximum load ($P = P_{max}$) and *J* was the value of the J-integral at fracture ($P = P_{fail}$). The detailed equations used to compute the stress-intensity *K* and the plastic component of *J* are provided in ASTM E1820 (ASTM 2005). Additionally, R-curve analysis was conducted on the BG/PUR composites. After correcting J-integral for crack extension, crack growth toughness was determined as the slope of *J* versus corresponding crack extensions (Fig. 10). Statistical significance between the means of parameters corresponding to each material tested was determined by a one-way ANOVA with Tukey honest significant difference (HSD).

2.5 SENB notch and fracture characterization

A Canon EOS 5D Digital SLR camera mounted with a macro photo lens MP-E 65mm 1:2.8 was used to qualitatively characterize the compressive fatigue tested specimens. Additionally, images of starter notch and subsequent crack propagation were taken in between loading cycles during fracture toughness mechanical testing by the SLR camera to qualitatively characterize stable and unstable crack extensions. Scanning electron microscope (SEM) imaging at 45X magnification and 5 kV (Hitachi S-4200 SEM (Finchampstead, UK)) was used to obtain fractography images of the internal cracked surface of specimens post fracture toughness mechanical testing.

3. Results

A summary of the groups tested in cyclic compressive fatigue, the corresponding maximum stress levels applied (σ_{max}), and cycle intervals between recorded cycles are shown in Table 1 (n=6 for each specimen and maximum stress level pairing). Cyclic compression test data for BG/PUR composites and CaS/P bone cement showed progressive loss of secant modulus (and thus broadening of hysteresis loop) and accumulation of residual strains (cyclic creep). For the PCL-BG/PUR composite and CaS/P cement groups (Fig. 1B and C, respectively), there was creep and damage accumulation (modulus loss) during a relatively long fatigue life, whereas U-BG/PUR composite showed primarily viscoelastic behavior over a short

fatigue life (Fig. 1D). Additionally, there was less overall creep exhibited by CaS/P cement compared to BG/PUR composites. Fatigue resistance of PCL-BG/PUR was superior to that of U-BG/PUR and CaS/P at the higher stress levels for each of fatigue failure definition: A) 10% decrease in secant modulus, B) 1% creep (c_k), C) 3% maximum displacement (d_m) (Fig. 2). Overall, the fatigue behavior of each sample type at each failure definition exhibited the expected linear relationship with a negative slope between the maximum stress level applied (σ_{max}) and fatigue life (log scale). At σ_{max}=5 MPa, surface-modified PCL-BG composites and the CaS/P cement had a similar fatigue life when failure was defined with respect to secant modulus degradation (damage), but the fatigue life was higher for PCL-BG than for CaS/P when failure was based on overall creep and maximum displacement (Fig. 2B and 2C). Unmodified BG/PUR composites had a substantially lower fatigue life for all definitions of failure compared to both the surface-modified BG composite and CaS/P cement (Fig. 2). In addition, the PCL-BG/PUR composite had longer fatigue life compared to the CaS/P cement at σ_{max} = 10–15 MPa irrespective of failure definition (Fig. 2). The median number of cycles until failure (creep-based failure definition) tested at σ_{max} = 5 MPa for PCL-BG/PUR composite, CaS/P cement, and U-BG/PUR composite was 230500, 23500, and 3, respectively (Table 2). The difference in fatigue life between PCL-BG/PUR composite and CaS/P cement was also statistically significant at higher loads of 10 and 15 MPa.

Creep strains developed throughout cyclic fatigue loading in force control, and PCL-BG/PUR composite and CaS/P cement exhibited the three stages of creep for a viscoelastic material: primary rapid strain increase in the first loading cycles, steady state-creep over the majority of the fatigue life, and a rapid increase in deformation near the end of the fatigue life (Fig. 3). The non-linear relationship between creep and loading cycle was similar between both surface-modified BG composites and CaS/P cements at σ_{max} = 5 MPa (Fig. 3A), but the CaS/P cement failed sooner and the steady state creep rate occurred at a higher stain than PCL-BG/PUR composite. This typical creep behavior was maintained with the surface-modified BG composite that was loaded at σ_{max} between 10–30 MPa (Fig. 3B) as well CaS/P cement loaded at σ_{max} of 10 and 15 MPa (Fig. 3C). After a specimen reached a creep of approximately 0.2 mm or strain of 1.7%, complete failure usually occurred shortly thereafter. Also at these stress levels, surface-modified BG composites showed a more gradual transition from the second to third stage of creep compared to the CaS/P cement (Fig. 3B vs. Fig. 3C). As for the U-BG/PUR composite, the steady creep state occurred at lower number of cycles and at higher strains leading to lower fatigue life compared to the other materials (Fig 3D vs. Fig. 3A). The modulus of both surface-modified BG/PUR composite and CaS/P cement degraded throughout the fatigue testing (Fig. 3E–F). The BG/PUR composite showed a steady decrease in modulus as creep occurred, while CaS/P cement maintained a stiff modulus (within a small range) until failure drastically reduced the overall modulus within a small amount of creep.

All specimens showed macroscopic failure at cycles exceeding those defined by failure mechanisms related to modulus, creep, and displacement, which is supported by images of tested specimens at strains >5% (Fig. 4A–C). PCL-BG composites stayed intact at these high strains, failing primarily at the specimen ends (Fig. 4A). CaS/P cement showed numerous cracking events throughout the gain region of the specimen, often crumbling apart

as fatigue loading completed (Fig. 4B). U-BG composites often failed in the gage region of specimen but usually disassembled in large fractures rather than complete crumbling (Fig. 4C).

To critically evaluate the fracture toughness of each material, we determined the stress intensity factor or resistance to crack initiation (K_{init}) and J-integral from the load vs. displacement curves (Fig. 5A–C). Images of the SENB specimen taken during fracture toughness testing revealed propagation of a crack from the micro-notches in PCL-BG composite and CaS/P cement (as indicated by white arrow in Fig. 5D–E, respectively). Cracking from the micro-notched was not observed for the exterior of the U-BG/PUR composite specimen, but failure did occur. Fracture toughness properties (K_{init} and J-integral) of PCL-BG composite were significantly higher compared to the other two groups (Table 3), but there was no significant differences between the U-BG composite and CaS/P cement. There was a sufficient number of crack events for only the U- and PCL-BG/PUR composites (i.e., rising R-curves behavior), allowing the crack growth toughness of these specimens to be determined. J-integral was plotted against crack extension (Fig. 6A). The surface modification of the BG before incorporation with the PUR binder significantly increased the elasto-plastic J-integral (Table 3) and change in J per crack extension (Fig. 6A). This crack growth toughness is not existent in the brittle CaS/P material because crack instability occurred early in the loading of SENB specimens. SEM images of fractured surfaces show that BG/PUR composites (Fig. 6B and D) had substantially rougher fracture surface than the CaS/P cement (Fig. 6C), suggesting a more tortuous path for crack propagation. No noticeable difference was observed between the fracture surfaces of the two BG/PUR composites tested.

4. Discussion

Injectable and settable bone grafts with bone-like mechanical properties have the potential to improve clinical management of fractures at weight-bearing sites. Previous studies reported that allograft/ or ceramic/polymer composites remodel and support new bone formation in preclinical models of bone regeneration in metaphyseal defects (Adhikari, Gunatillake et al. 2008, Dumas, Davis et al. 2010, Dumas, Zienkiewicz et al. 2010, Yoshii, Dumas et al. 2012, Harmata, Ward et al. 2014). While PCL-BG/polymer composites exhibited torsional strengths exceeding those of trabecular bone and supported new bone growth when injected into femoral condyle defects in rats (Harmata, Ward et al. 2014), their mechanical properties under dynamic loadings have not been investigated. In this study, we measured the fatigue and fracture toughness properties of U-BG and PCL-BG/polymer composites, as well as an injectable CPC clinical control (CaS/P). While U-BG composites had torsional strength (Harmata, Ward et al. 2014) and K_{init} values equal to ~35% of those measured for PCL-BG composites, the fatigue life of U-BG composites was almost 10^5 times shorter than that measured for PCL-BG composites at a 5 MPa. Similarly, CaS/P showed torsional strength (Dumas, Prieto et al. 2014) and K_{init} values equal to ~20% of the values measured for PCL-BG composites, but the fatigue life of CaS/P was 10^4 shorter at 15 MPa. These observations underscore the importance of fatigue testing under dynamic loads to assess the weight-bearing potential of bone graft substitutes, since materials with similar quasi-static compressive modulus and strength can show dramatic differences in fatigue properties.

A limited number of studies have evaluated dynamic compressive mechanical properties of resorbable synthetic biomaterials for orthopaedic applications. Calcium silicate-gelatin composites were reported to have fatigue life ranging from 10^3–10^5 at a 30 MPa load (Ding, Wei et al. 2011). Additionally, 13–93 bioactive glass scaffolds made by robotic deposition were reported to have fatigue lives ranging from 10^4–10^6 at loads from 10–30 MPa (Liu, Rahaman et al. 2013). Although the fatigue lives of these synthetic biomaterials are slightly longer than the PCL-BG composite in this study, they are not injectable or settable. The compressive fatigue life of non-resorbable acrylic bone cements (e.g., PMMA) indicated for structural repair of bone has been shown to be 10^3–10^6 at maximum compressive strengths of approximately 13 – 60 MPa at 2 Hz (Jaffe, Rose et al. 1974, Krause and Mathis 1988). Note that numerous intrinsic and extrinsic affect the fatigue life of PMMA (Lewis 2003, Ajaxon and Persson 2014). Thus, surface polymerization of PCL on the BG surface increased the fatigue life of the PCL-BG composites to values approaching that of structural acrylic cement when tested in compression mode.

The compressive fatigue mechanical properties of both human cortical and trabecular bone display S-N curves with N_f increasing with decreasing applied stress (Rapillarda, Charlebois et al. 2006, Kruzic and Ritchie 2008), as observed for all synthetic bone grafts tested in the present study. PCL-BG/polymer composites exhibited compressive fatigue properties in the range of human trabecular bone tested at physiological and supra-physiological loads (Haddock, Yeh et al. 2004, Rapillard, Charlebois et al. 2006, Dendorfer, Maier et al. 2008), but not those of cortical bone (Caler and Carter 1989, Zioupos, Gresle et al. 2008). CaS/P cement and U-BG/polymer composite did not exhibit compressive fatigue properties in the range of either bone type. PCL-BG composite had an N_f in the range of 10^2–10^4 (Fig. 2A) for maximum stress levels of 15–30 MPa (modulus-based failure definition, as was used in comparative human bone studies). These stress levels are equivalent to normalized loads of $\log(\sigma/\text{averaged } E_0) = -2.37$ to -2.6. In two previous studies, human vertebral trabecular bone (independently tested healthy and elderly patients) was mechanically tested in dynamic compression fatigue over a range of σ/E_0 values that corresponded to maximum stress levels between 15–30 MPa. The published fatigue lives or these human specimens ranged from approximately 10^2–10^4 (Dendorfer, Maier et al. 2008) and 10^2–10^5 (Haddock, Yeh et al. 2004) for healthy and elderly patients, respectively. Although it has been shown that higher frequency of applied load increases N_f (Kruzic and Ritchie 2008, Diel, Huber et al. 2012), the sinusoidal frequency of loading applied in our study (5 Hz) was not much higher than the human studies referenced (1.32–2.87 Hz and 0.9–3 Hz, respectively). The PCL-BG composite N_f exceeded values published in the former study (Haddock, Yeh et al. 2004). Thus, we anticipate that an increase in frequency from 2–3 Hz to 5 Hz does not prevent the appropriate comparison to these human bone studies.

The creep behavior shown for BG/PUR composites during fatigue testing (Fig. 3) matched characteristic creep profiles shown for these human bone specimens. Human specimens were shown to fail not only from modulus degradation but also from height subsidence, which motivated including the creep- and displacement-based failure definitions within the analysis of this study. During applied maximum stress levels of 10–30 MPa, PCL-BG composites exhibited steady state creep during strains from 0.8–1.5% (c_k=0.1–0.2 mm).

Previous studies showed human trabecular bone exhibited steady creep during strains <0.6% (Haddock, Yeh et al. 2004, Dendorfer, Maier et al. 2008). Thus, PCL-BG/PUR composite can withstand creep strain equal to or higher than human trabecular bone before entering the third stage of typical creep behavior.

The fracture toughness properties determined for the PCL-BG/PUR composite (K_{init} =1.43 MPa $m^{0.5}$, Table 3) were comparable to published values for bone and related orthopaedic biomaterials. For Mode I testing (crack opening under tensile stress), wet trabecular and cortical bone have been shown to have ranges of K_{IC} = 0.1 – 0.8 MPa $m^{0.5}$ (Oyen 2008, Fu, Saiz et al. 2011) and 2 – 12 MPa $m^{0.5}$ (Melvin 1993, Morgan, Yetkinler et al. 1997, Cook and Zioupos 2009 , Fu, Saiz et al. 2011, Granke, Makowski et al. 2015), respectively. The K_{IC} for six commercially available non-resorbable bone cements and poly(methyl methacrylate) (PMMA) ranged from 1.03 – 2.32 MPa $m^{0.5}$ (Gilbert, Ney et al. 1995, Lewis 2006). For CaS/P cement, K_{init}=0.32 MPa $m^{0.5}$ (Table 3) was comparable to the K_{IC} of another calcium phosphate cement (Norian Skeletal Repair System, SRS®) previously reported (K_{IC}=0.14 MPa $m^{0.5}$) (Lewis 2006). Despite having a similar carbonated apatite composition to the mineral phase of bone, Norian SRS® and CaS/P cements showed considerably lower toughness compared to that of wet bone. Thus, the PCL-BG/polymer composite has fracture toughness properties exceeding that of resorbable CPCs and approaching the low end of the range for cortical bone and structural acrylic bone cements.

Fatigue creep and fracture toughness results from this study provide mechanistic insight regarding the longer fatigue life of PCL-BG/polymer composite compared to CaS/P cement. PCL-BG composite showed several stable cracking events throughout the fracture toughness testing (Fig. 5A), whereas CaS/P did not show signs of stable cracking but rather unstable cracking when an event was observed (Fig. 5B). Although the PCL-BG composite is not immune to microcrack formation, this damage appears to be constrained to small areas of the composite. This finding is supported by images of composites after complete fatigue failure that showed signs of shear bands with the majority of the composite intact (Fig. 4A), whereas the CaS/P cement showed numerous end-to-end catastrophic cracks throughout the specimen (Fig. 4B). CaS/P cement appeared to have better resistance to initial creep deformation compared to PCL-BG composite at loads above 5 MPa (Fig. 3C), but complete failure occurred at lower overall creep and appeared to happen more rapidly (Fig. 3 E and F). Thus it appears CaS/P cannot absorb loaded energy in a stable manner. When microcracks formed, these unstable events led to failure of the CaS/P, presumably due to its low fracture toughness.

A recent review reported that the majority of calcium phosphate/polymer composites had quasi-static compressive mechanical properties below those of human trabecular bone and bulk monolithic calcium phosphates (Johnson and Herschler 2011). The reason for these sub-optimal mechanical properties may be due to poor interfacial bonding between phases within the composite. Adequate interfacial bonding is necessary in order to capitalize on the potential benefits of combining a tough ductile polymer phase with a strong brittle phase. The high fracture toughness of bone has been attributed to a number of factors including interfacial bonding between the collagen and apatite phases (Wang 2003, Wegst, Bai et al. 2015). Similarly, the superior fatigue and fracture toughness properties of PCL-BG

composites are conjectured to result from interfacial bonding due to physical entanglements between surface-polymerized PCL chains on the BG particles and the continuous PUR network (Harmata, Ward et al. 2014).

To our knowledge, the surface-modified BG/PUR composite from the current study is the first published injectable, settable, and resorbable, synthetic bone graft with initial quasi-static and dynamic compressive mechanical properties equal to or greater than that of native trabecular bone. Considering that PCL-BG composites resorb and remodel *in vivo* (Harmata, Ward et al. 2014), their properties are anticipated to change with time. Consequently, it is important to verify that PCL-BG composites completely fill the defect and maintain sufficient fatigue resistance and fracture toughness properties throughout all stages of remodeling. The rate of BG dissolution is also an important factor regulating remodeling. Although 45S5 bioactive glass has been approved for commercial use by the FDA, future composite formulations may be improved by the inclusion of a more slowly degrading bioactive glass, such as 13–93, which may have prolonged a buffering affect (Jones 2013). Since BG dissolution and hydroxyapatite formation proceed in a basic environment (Jones 2013), increases in the local pH as the composite remodels are conjectured to buffer the acid-catalyzed degradation of poly(ester urethanes) (Hafeman, Li et al. 2008, Dumas, Prieto et al. 2014) (Antheunis, van der Meer et al. 2009) (Vert, Li et al. 1992). These questions are currently under investigation in a large animal load-bearing model of bone regeneration.

5. Conclusions

In this study, the dynamic compressive fatigue properties of BG/polymer composites when subjected to physiological or supra-physiological loads were evaluated, and their properties were compared to those of a commercially available biphasic CPC (CaS/P). Poly(ε-caprolactone) surface-modified BG/polymer composite fatigue resistance was superior to that of CaS/P cement at low and high compressive stress. The fatigue failures of BG/PUR composite and CaS/P biomaterials included both creep and damage accumulation. CaS/P cement reached steady state creep during fatigue testing at a higher stain than PCL-BG/polymer composite but showed catastrophic failure at a lower strain. Additionally, the fracture toughness properties of BG/polymer composites and CaS/P cements were evaluated. PCL surface modified BG/polymer composite showed significantly higher resistance to crack growth than CaS/P and un-modified BG/polymer composite groups.

Acknowledgements

This material is based upon work supported by the National Science Foundation under (Grant No. 0847711) (CAREER award to S.A. Guelcher) and the National Institutes of Health through the National Institute of Arthritis and Musculoskeletal and Skin Diseases under Award Number AR064304 (S.A. Guelcher and J. C. Wenke) and AR063157 (J.S. Nyman). The content is solely the responsibility of the authors and does not necessarily represent the official views of the National Institutes of Health. A.J. Harmata acknowledges financial support from an Oak Ridge Institute for Science and Education Fellowship funded by the U.S. Army Medical Research and Materiel Command.

Abbreviations

LTI	lysine triisocyanate

BG	45S5 bioactive glass
CaS/P	calcium sulfate and phosphate-based bone cement
PCL-BG/PUR	poly(ε-caprolactone) surface-modified BG and polyurethane composite
U-BG/PUR	un-modified BG and polyurethane composite
σ_{max}	maximum stress level applied
c_k	overall creep strain (relative to initial strain)
d_m	maximum displacement
K_{init}	critical stress intensity required to initiate cracks

References

Adhikari R, Gunatillake PA, Griffiths I, Tatai L, Wickramaratna M, Houshyar S, Moore T, Mayadunne RTM, Field J, McGee M, Carbone T. Biodegradable injectable polyurethanes: Synthesis and evaluation for orthopaedic applications. Biomaterials. 2008; 29(28):3762–3770. [PubMed: 18632149]

Ajaxon I, Persson C. Compressive fatigue properties of a commercially available acrylic bone cement for vertebroplasty. Biomechanics and Modeling in Mechanobiology. 2014; 13(6):1199–1207. [PubMed: 24659042]

Anderson DD, Van Hofwegen C, Marsh JL, Brown TD. Is elevated contact stress predictive of post-traumatic osteoarthritis for imprecisely reduced tibial plafond fractures? J Orthop Res. 2011; 29(1): 33–39. [PubMed: 20607840]

Antheunis H, van der Meer J-C, de Geus M, Kingma W, Koning CE. Improved Mathematical Model for the Hydrolytic Degradation of Aliphatic Polyesters. Macromolecules. 2009; 42(7):2462–2471.

ASTM. Designation: E 1820, Standard Test Method for Measurement of Fracture Tougness. ASTM International. 2005

ASTM. Designation F2118-10. Standard Test Method for Constant Amplitude of Force Controlled Fatigue Testing of Acrylic Bone Cement Materials. ASTM International. 2010

Bohner M. Design of Ceramic-Based Cements and Putties for Bone Graft Substitution. European Cells & Materials. 2010; 20:1–12. [PubMed: 20574942]

Bosse MJ, MacKenzie EJ, Kellam JF, Burgess AR, Webb LX, Swiontkowski MF, Sanders RW, Jones AL, McAndrew MP, Patterson BM, McCarthy ML, Travison TG, Castillo RC. An analysis of outcomes of reconstruction or amputation after leg-threatening injuries. N Engl J Med. 2002; 347(24):1924–1931. [PubMed: 12477942]

Caler WE, Carter DR. Bone Creep-Fatigue Damage Accumulation. Journal of Biomechanics. 1989; 22(6–7):625–635. [PubMed: 2808445]

Chan C, Thompson I, Robinson P, Wilson J, Hench L. Evaluation of Bioglass/dextran composite as a bone graft substitute. International Journal of Oral and Maxillofacial Surgery. 2002; 31(1):73–77. [PubMed: 11936404]

Cook RB, Zioupos P. The fracture toughness of cancellous bone. Journal of Biomechanics. 2009; 42(13):2054–2060. [PubMed: 19643417]

Dendorfer S, Maier HJ, Taylor D, Hammer J. Anisotropy of the fatigue behaviour of cancellous bone. Journal of Biomechanics. 2008; 41(3):636–641. [PubMed: 18005974]

Diel S, Huber O, Saage H, Steinmann P, Winter W. Mechanical behavior of a cellular composite under quasi-static, static, and cyclic compression loading. Journal of Materials Science. 2012; 47(15): 5635–5645.

Ding S-J, Wei C-K, Lai M-H. Bio-inspired calcium silicate-gelatin bone grafts for load-bearing applications. Journal of Materials Chemistry. 2011; 21(34):12793–12802.

Dumas JE, BrownBaer PB, Prieto EM, Guda T, Hale RG, Wenke JC, Guelcher SA. Injectable reactive biocomposites for bone healing in critical-size rabbit calvarial defects. Biomedical Materials. 2012; 7(2)

Dumas JE, Davis T, Holt GE, Yoshii T, Perrien DS, Nyman JS, Boyce T, Guelcher SA. Synthesis, characterization, and remodeling of weight-bearing allograft bone/polyurethane composites in the rabbit. Acta Biomaterialia. 2010; 6(7):2394–2406. [PubMed: 20109586]

Dumas JE, Prieto EM, Zienkiewicz KJ, Guda T, Wenke JC, Bible J, Holt GE, Guelcher SA. Balancing the Rates of New Bone Formation and Polymer Degradation Enhances Healing of Weight-Bearing Allograft/Polyurethane Composites in Rabbit Femoral Defects. Tissue Engineering Part A. 2014; 20(1–2):115–129. [PubMed: 23941405]

Dumas JE, Zienkiewicz K, Tanner SA, Prieto EM, Bhattacharyya S, Guelcher SA. Synthesis and Characterization of an Injectable Allograft Bone/Polymer Composite Bone Void Filler with Tunable Mechanical Properties. Tissue Engineering Part A. 2010; 16(8):2505–2518. [PubMed: 20218874]

Evaniew N, Tan V, Parasu N, Jurriaans E, Finlay K, Deheshi B, Ghert M. Use of a calcium sulfate-calcium phosphate synthetic bone graft composite in the surgical management of primary bone tumors. Orthopedics. 2013; 36(2):e216–e222. [PubMed: 23380017]

Fu Q, Saiz E, Rahaman MN, Tomsia AP. Bioactive glass scaffolds for bone tissue engineering: state of the art and future perspectives. Materials Science & Engineering C-Materials for Biological Applications. 2011; 31(7):1245–1256.

Gilbert JL, Ney DS, Lautenschlager EP. Self-reinforced composite poly(methyl methacrylate): static and fatigue properties. Biomaterials. 1995; 16(14):1055.

Gisep A, Kugler S, Wahl D, Rahn B. Mechanical characterisation of a bone defect model filled with ceramic cements. Journal of Materials Science-Materials in Medicine. 2004; 15(10):1065–1071. [PubMed: 15516866]

Granke M, Makowski A, Uppuganti S, Does M, Nyman J. Identifying novel clinical surrogates to assess human bone fracture toughness. J. Bone Miner. 2015; 30(7):1290–1300.

Guelcher SA, Patel V, Gallagher KM, Connolly S, Didier JE, Doctor JS, Hollinger JO. Synthesis and in vitro biocompatibility of injectable polyurethane foam scaffolds. Tissue Engineering. 2006; 12(5):1247–1259. [PubMed: 16771638]

Haddock SM, Yeh OC, Mummaneni PV, Rosenberg WS, Keaveny TM. Similarity in the fatigue behavior of trabecular bone across site and species. Journal of Biomechanics. 2004; 37(2):181–187. [PubMed: 14706320]

Hafeman AE, Li B, Yoshii T, Zienkiewicz K, Davidson JM, Guelcher SA. Injectable biodegradable polyurethane scaffolds with release of platelet-derived growth factor for tissue repair and regeneration. Pharmaceutical Research. 2008; 25(10):2387–2399. [PubMed: 18516665]

Hall JA, Beuerlein MJ, McKee MD. Open reduction and internal fixation compared with circular fixator application for bicondylar tibial plateau fractures. Surgical technique. J Bone Joint Surg Am 91 Suppl 2 Pt. 2009; 1:74–88.

Harmata AJ, Ward CL, Zienkiewicz K, Wenke JC, Guelcher SA. Investigating the Effects of Surface-Initiated Polymerization of ε-Caprolactone to Bioactive Glass Particles on the Mechanical Properties of Settable Polymer/Ceramic Composites. Journal of Materials Research. 2014; 29(20): 2398–2407. [PubMed: 25798027]

Jaffe WL, Rose RM, Radin EL. On the Stability of the Mechanical Properties of Self-curing Acrylic Bone Cement. Journal of bone and Joint Surgery. 1974; 56(8):1711–1714. [PubMed: 4474043]

Jiang G, Walker GS, Jones IA, Rudd CD. XPS identification of surface-initiated polymerisation during monomer transfer moulding of poly(epsilon-caprolactone)/Bioglass (R) fibre composite. Applied Surface Science. 2005; 252(5):1854–1862.

Johnson AJW, Herschler BA. A review of the mechanical behavior of CaP and CaP/polymer composites for applications in bone replacement and repair. Acta Biomaterialia. 2011; 7(1):16–30. [PubMed: 20655397]

Jones JR. Review of bioactive glass: From Hench to hybrids. Acta Biomaterialia. 2013; 9(1):4457–4486. [PubMed: 22922331]

Kessler MR, Sottos NR, White SR. Self-healing structural composite materials. Composites Part a-Applied Science and Manufacturing. 2003; 34(8):743–753.

Krause W, Mathis RS. Fatigue Properties of Acrylic Bone Cements - Review of the Literature. Journal of Biomedical Materials Research-Applied Biomaterials. 1988; 22(A1):37–53. [PubMed: 3286653]

Kruzic JJ, Ritchie RO. Fatigue of mineralized tissues: Cortical bone and dentin. Journal of the Mechanical Behvaior of Biomedical Materials. 2008; 1(1):3–17.

Latour RA, Black J. Development of Frp Composite Structural Biomaterials -Fatigue-Strength of the Fiber-Matrix Interfacial Bond in Simulated in-Vivo Environments. Journal of Biomedical Materials Research. 1993; 27(10):1281–1291. [PubMed: 8245042]

Lewis G. Fatigue testing and performance of acrylic bone-cement materials: State-of-the-art review. Journal of Biomedical Materials Research Part B: Applied Biomaterials. 2003; 66B(1):457–486.

Lewis G. Injectable bone cements for use in vertebroplasty and kyphoplasty: State-of-the-art review. Journal of Biomedical Materials Research Part B-Applied Biomaterials. 2006; 76B(2):456–468.

Liu X, Rahaman MN, Hilmas GE, Bal BS. Mechanical properties of bioactive glass (13–93) scaffolds fabricated by robotic deposition for structural bone repair. Acta Biomaterialia. 2013; 9(6):7025–7034. [PubMed: 23438862]

Malinin TI, Carpenter EM, Temple HT. Particulate bone allograft incorporation in regeneration of osseous defects; importance of particle sizes. The Open Orthopaedics Journal. 2007; 1:19–24. [PubMed: 19471600]

Melvin JW. Fracture-Mechanics of Bone. Journal of Biomechanical Engineering-Transactions of the Asme. 1993; 115(4):549–554.

Morgan EF, Yetkinler DN, Constantz BR, Dauskardt RH. Mechanical properties of carbonated apatite bone mineral substitute: strength, fracture and fatigue behaviour. Journal of Materials Science-Materials in Medicine. 1997; 8(9):559–570. [PubMed: 15348708]

Moseley J, Blum B. PRO-DENSE® injectable regenerative graft: In vitro and in vivo observations, and a proposed mechanism of action. Wright Medical Technology, Inc. 2008

Musahl V, Tarkin I, Kobbe P, Tzioupis C, Siska PA, Pape H-C. New trends and techniques in open reduction and internal fixation of fractures of the tibial plateau. The Journal of Bone & Joint Surgery. 2009; 91B(4):426–433. [PubMed: 19336799]

Oyen ML. The materials science of bone: Lessons from nature for biomimetic materials synthesis. MRS Bulletin. 2008; 33(1):49–55.

Papagelopoulos PJ, Partsinevelos AA, Themistocleous GS, Mavrogenis AF, Korres DS, Soucacos PN. Complications after tibia plateau fracture surgery. Injury. 2006; 37:475–484. [PubMed: 16118010]

Pinter G, Ladstätter E, Billinger W, Lang RW. Characterisation of the tensile fatigue behaviour of RTM-laminates by isocyclic stress-strain-diagrams. International Journal of Fatigue. 2006; 28(10): 1277–1283.

Ramakrishna S, Mayer J, Wintermantel E, Leong KW. Biomedical applications of polymer-composite materials: a review. Composites Science and Technology. 2001; 61(9):1189–1224.

Rapillard L, Charlebois M, Zysset PK. Compressive fatigue behavior of human vertebral trabecular bone. Journal of Biomechanics. 2006; 39(11):2133–2139. [PubMed: 16051256]

Rapillarda L, Charlebois M, Zysset PK. Compressive fatigue behavior of human vertebral trabecular bone. Journal of Biomechanics. 2006; 39(11):2133–2139. [PubMed: 16051256]

Rezwan K, Chen QZ, Blaker JJ, Boccaccini AR. Biodegradable and bioactive porous polymer/inorganic composite scaffolds for bone tissue engineering. Biomaterials. 2006; 27(18):3413–3431. [PubMed: 16504284]

Ritchie RO, Koester KJ, Ionova S, Yao W, Lane NE, Ager JW III. Measurement of the toughness of bone: A tutorial with special reference to small animal studies. Bone. 2008; 43(5):798–812. [PubMed: 18647665]

Schatzker J, McBroom R, Bruce D. The tibial plateau fracture: the Toronto experience 1968–1975. Clinical Orthopaedics and Related Research. 1976; (138):94–104. [PubMed: 1261139]

Simpson D, Keating JF. Outcome of tibial plateau fractures managed with calcium phosphate cement. Injury. 2004; 35(9):913–918. [PubMed: 15302246]

Slane J, Vivanco J, Meyer J, Ploeg H-L, Squire M. Modification of acrylic bone cement with mesoporous silica nanoparticles: Effects on mechanical, fatigue and absorption properties. Journal of the Mechanical Behavior of Biomedical Materials. 2014; 29:451–461. [PubMed: 24211354]

Tilbrook MT, Moon RJ, Hoffman M. Crack propagation in graded composites. Composites Science and Technology. 2005; 65(2):201–220.

Verne E, Vitale-Brovarone C, Bui E, Bianchi CL, Boccaccini AR. Surface functionalization of bioactive glasses. Journal of Biomedical Materials Research Part A. 2009; 90B(4):981–992. [PubMed: 18655138]

Vert M, Li S, Spenlehauer G, Guerin P. Bioresorbability and biocompatibility of aliphatic polyesters. Journal of Materials Science: Materials in Medicine. 1992; 3(6):432–446.

Wang M. Developing bioactive composite materials for tissue replacement. Biomaterials. 2003; 24(13):2133–2151. [PubMed: 12699650]

Wegst UG, Bai H, Saiz E, Tomsia AP, Ritchie RO. Bioinspired structural materials. Nature Materials. 2015; 14(1):23–36. [PubMed: 25344782]

Yoshii T, Dumas JE, Okawa A, Spengler DM, Guelcher SA. Synthesis, characterization of calcium phosphates/polyurethane composites for weight-bearing implants. Journal of Biomedical Materials Research Part B-Applied Biomaterials. 2012; 100B(1):32–40.

Young MJ, Barrack RL. Complications of internal fixation of tibial plateau fractures. Orthopedic Reviews. 1994; 23:149–154.

Zioupos P, Gresle M, Winwood K. Fatigue strength of human cortical bone: Age, physical, and material heterogeneity effects. Journal of Biomedical Materials Research Part A. 2008; 86(3):627–636. [PubMed: 18022837]

Highlights

- Surface-modified bioglass composite had longer fatigue life than calcium-phosphate cement.
- Fatigue failure of composite and cement included both creep and damage accumulation.
- Steady state creep of cement at low stress occurred over higher strain range than composite.
- Crack initiation toughness was significantly higher for composite than for cement.
- PCL-BG/PUR composite is a potential synthetic bone graft for regions under dynamic loading.

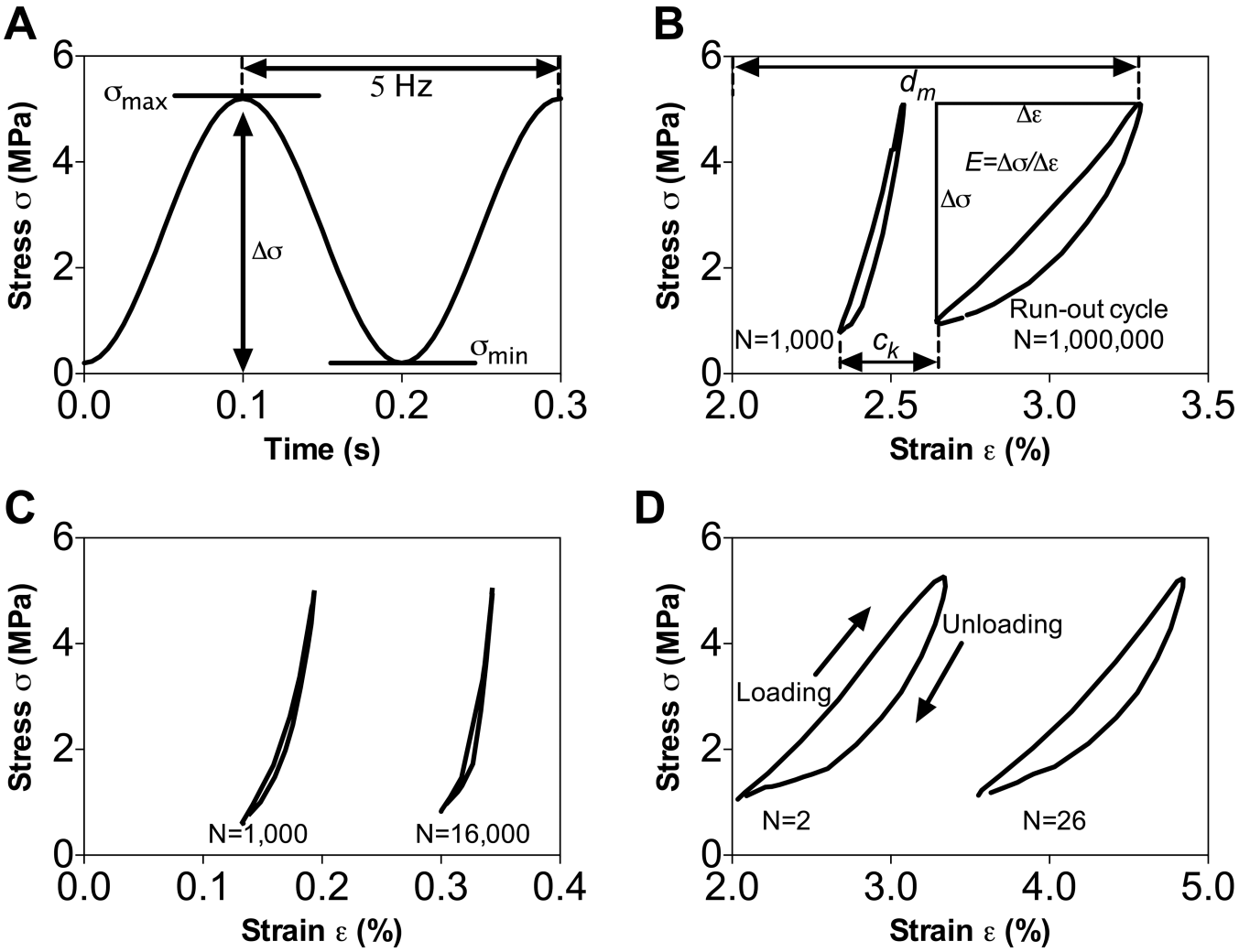

Figure 1.

Compressive fatigue method and analysis. (A) Sinusoidal loading details for a maximum stress applied (σ_{max})=5 MPa and frequency=5 Hz. Representative stress (σ) vs. strain (s) curves (σ_{max} =5 MPa), first and last cycles recorded, for (B) PCL surface-modified 45S5 bioactive glass (BG) and polyurethane composite (PCL-BG/PUR), (C) calcium sulfate and phosphate-based bone cement (CaS/P), and (D) un-modified BG and PUR composite (U-BG/PUR). Included in panel B), secant modulus (*E*) was defined at change in stress (Δσ), divided by the change in strain (Δε), between the lowest and highest strain during loading. Creep strain (c_k) and maximum displacement (d_m) were defined by translation along the x-axis.

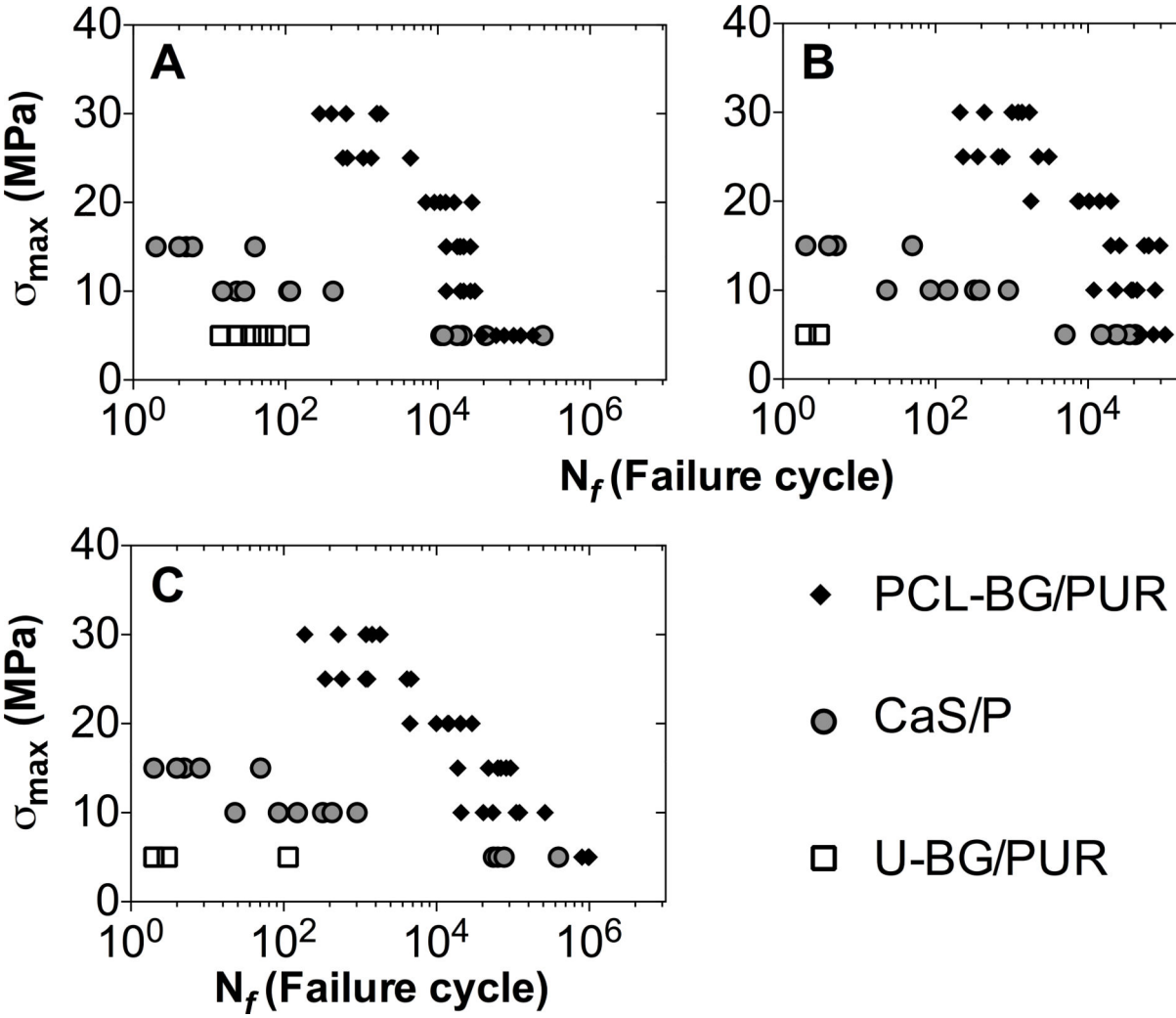

Figure 2.

Fatigue S-N plot of BG/PUR composites and CaS/P cement. Fatigue life (N_f) was determined based on three different definitions of failure cycle, as the first cycle with (A) 10% decrease in secant modulus (E) compared to average of first 10 segments, (B) 1% creep deformation (c_k), and (C) 3% maximum displacement (d_m). Data shown includes n=6 for each load/specimen group.

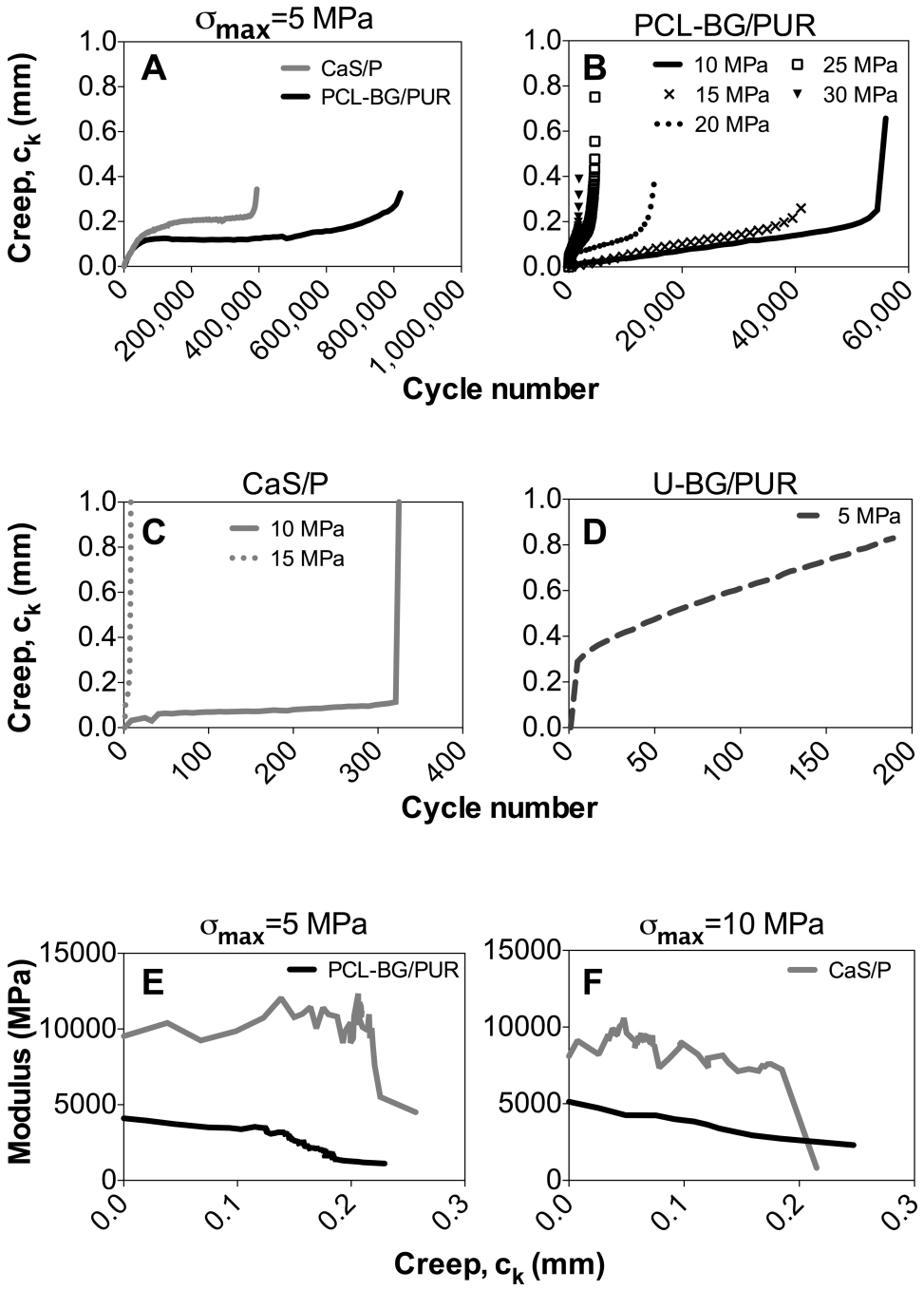

Figure 3.

Fatigue testing creep (c_k) behavior vs. cycle number. Tested at maximum stress level (σ_{max}) of (A) 5 MPa for PCL-BG/PUR composite and CaS/P cement, (B) 10-30MPa for PCL-BG/PUR, and (C) 10–15 MPa for CaS/P, and (D) 5 MPa for U-BG/PUR. Plots shown are median, representative data of each specimen group/load group (n=6). Note that differences between the groups/stress levels in the value of the final creep data point plotted were due to interval span of cyclic data collected. Modulus (*E*) vs. creep (c_k) for PCL-BG/PUR and CaS/P at σ_{max}= (E) 5 MPa and (F) 10 MPa.

Figure 4.

Macroscopic specimen failure. Images of specimens post-fatigue testing (strain= 5%): (A) PCL-BG/PUR, (B) CaS/P, and (C) U-BG/PUR. Centimeter ruler shown in images.

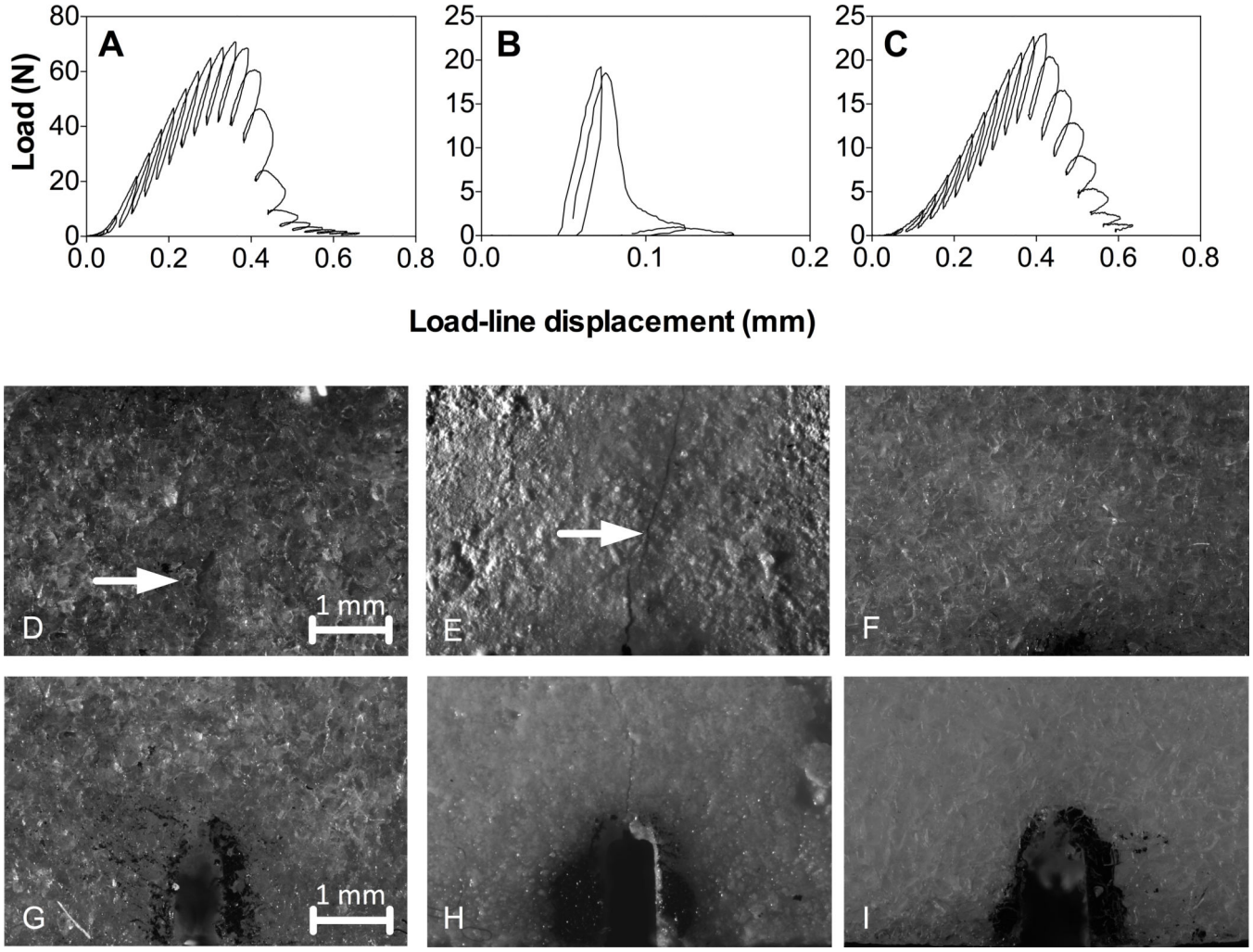

Figure 5.

Fracture toughness testing. Applied load vs. load-line displacement curves for (A) PCL-BG/PUR, (B) CaS/P, and (C) U-BG/PUR. Images of representative typical crack propagation for each group (n=3) during fracture toughness testing. Displayed images respectively show above/include the starter notch for (D/G) PCL-BG/PUR, (E/H) CaS/P, and (F/I) U-BG/PUR. White arrows point to propagated crack. All images were taken at the same magnification. Scale bar indicates 1 mm.

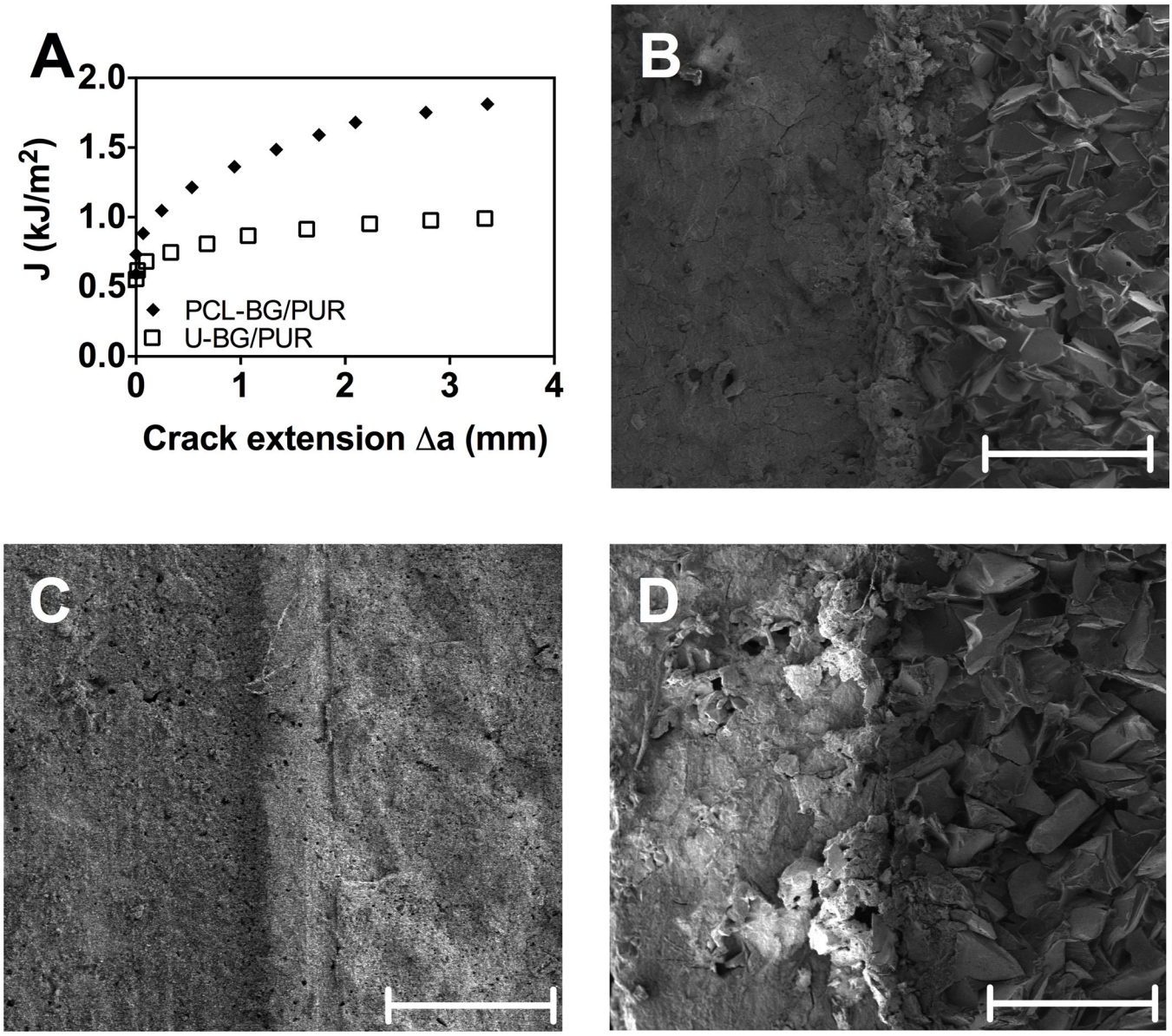

Figure 6.

Fracture toughness analysis. Plot of (A) *J* vs. crack extension for PCL-BG and U-BG/PUR composites. SEM images of pre-cut micro-notch (left half of image) and interior of cracked specimen (right half of image) for (B) PCL-BG/PUR, (C) CaS/P, and (D) U-BG/PUR, after fracture toughness testing. Scale bar indicates 667 μm.

Table 1

Compressive fatigue study design. The numbers corresponding to each maximum stress applied (σ_{max}) and specimen tested refer to the interval length (number of cycles) between recorded cycles. '-' indicates the specimen was not subjected to corresponding stress.

σ_{max} (MPa)	PCL-BG/PUR	CaS/P	U-BG/PUR
5	1000	1000	1
10	1000	1	-
15	1000	1	-
20	10	-	-
25	10	-	-
30	1	-	-

Table 2

Median fatigue life (N_f) based on 1% creep failure definition, at maximum stress applied (σ_{max}). Values reported as 'median (n=6), (25% percentile, 75% percentile).' '-' indicates the specimen was not subjected to corresponding stress. Mann-Whitney tests were performed to determine statistical significance between the mean of groups.

σ_{max} (MPa)	PCL-BG/PUR	CaS/P	U-BG/PUR
5	230500[a] (66500, 495000)	23500 (12500, 36750)	3 (2, 3) [ab]
10	38000[a] (20250, 52000)	236 (70, 511)	-
15	58500[a] (24500, 69250)	4 (3, 16)	-
20	9075 (5960, 15735)	-	-
25	710 (327, 2443)	-	-
30	1115 (383, 1458)	-	-

[a] $p<.0022$, at specific σ_{max} relative to to CaS/P.

[b] $p<.0022$, at specific σ_{max} relative to to PCL-BG/PUR.

Table 3

Fracture toughness properties. Statistical significance of quantified value compared to the other groups determined by one-way ANOVA and Tukey HSD. Data shown is mean ± standard deviation (n=3).

Material	K_{init} (MPa m^0.5)	J (N/mm)
PCL-BG/PUR	1.43 ± 0.04[a]	1.54 ± 0.10[a]
CaS/P	0.32 ± 0.04	0.03 ± 0.01
U-BG/PUR	0.48 ± 0.07	0.62 ± 0.10

[a] $p<.05$, relative to either remaining material group.